

## MECHANICAL AND THERMO-MECHANICAL PROPERTIES OF HYBRID COMPOSITES PRODUCED FROM PALM FRUITS WASTES

Kumaden Kuncy IKPAMBESE<sup>1,\*</sup>, Cedrick Chiahemba IMADU<sup>2</sup>

<sup>1</sup>Department of Mechanical Engineering, University of Agriculture, P.M.B. 2373, Makurdi-Nigeria

<sup>2</sup>Chevron Nigeria Ltd Warri

---

### Abstract

*The mechanical and thermo-properties of hybrid composites produced from palm kernel fibres and palm kernel shells were determined. The palm wastes of three different sieve sizes (75 µm, 150 µm and 300 µm) were blended in the weight ratios (fibre/kernel) of 50:50. Composites were produced at 10 wt%, 20 wt%, 30 wt%, 40 wt% and 50 wt% particulate reinforcement after which mechanical and thermo-mechanical properties were determined. A total of fifteen samples were produced, five representing each sieve size using hand lay-up method with epoxy-resin as a binder. The particle size and particulate reinforcement were seen to affect the physical, mechanical and thermo-mechanical properties of the hybrid samples produced. The overall result of water taken in by the samples showed that 300 µm absorbed the highest water, while 75 µm had the least density. Sample from 300 µm particle size with 10 % particulate reinforcement gave the optimum Young modulus and flexural strength values of 89.277 MPa and 10.7760 MPa. The optimum value of impact strength was given by sample B (300 µm particle size) with 20 % particulate reinforcement was 10000 J/m<sup>2</sup>. It can be concluded that hybrid composites produced from palm kernel fibre and palm kernel shell can be utilized as materials for car bumper, interior decoration in automobile industries.*

**Keywords:** Particle size, particulate reinforcement, hybrid composite, physical and mechanical properties.

---

### Introduction

Hybrid composites are products of conglomerating more than one fibre or matrix (binder) [1]. The idea of hybridization is to provide the design engineer with choice of the material properties in order to meet a particular requirements, as the performance of the hybrid composites appear to have a weighted sum of the contributions of the individual components which normally give a balance between their advantages and disadvantages. According to Pothan *et al.* (2010) bio-fibres are gaining acceptance in several technological fields because of their desirable properties.

The current environmental awareness as a result of harmful effects of synthesized fibre and in addition with societal needs has given rise to the use of more than one organic fibre in composite production. Several studies have been carried out by researchers to determine the performance properties of hybrid composites.

Romomazini *et al.* [3] investigated performance properties (physical, mechanical and dynamic mechanical) of hybrid composites produced from glass and ramie fibers. The glass–ramie volume fractions with the overall fiber content of 10, 21 and 31 vol.% was used. The samples with higher ramie fiber contents gave hybrid composites with lower weight resulting in higher water absorbed into the samples. In another study, Eng *et al.* (2014) investigated the effects of combining silane treated oil palm fibre with polylactic acid to produce a hybrid composites. The samples were prepared by melting technique and the samples were characterized using

Fourier transform infrared (FTIR), thermogravimetric analysis (TGA), and scanning electron microscopy (SEM) incorporation of silane treated palm oil fiber improved the performance properties of unmodified OPMF hybrid composites. Flexural and impact strengths were enhanced by 17.60% and 48.43%, respectively.

Venkatachalam et al [1] studied the tensile strength of hybrid composites reinforced with natural and synthetic fibres. The samples were reinforced with two different fibers (jute and Gongura) using cashew nut shell resins as binder. The hybrid samples were evaluated to study the influence of various fiber parameters on mechanical strength. The authors noted that for better improvement in the performance properties the hybrid should be done at low volume. Pickering *et al.* [5] while investigating change in performance properties (tensile, flexural and impact strengths) of hybrid composites produced from kenaf and pineapple leaf fibre reinforced with high-density polyethylene (HDPE). The authors concluded that pineapple leaf fibre improved the tensile and flexural strength while kenaf improved impact strength and reduced water intake.

The mechanical properties of sisal fibre hybridized with bamboo fibre for the production of composites was investigated by [6]. Results showed that performance properties (tensile, and water intake) were found to decrease with the addition of up to 50 % bamboo fibre in sisal (unsaturated polyester as binder). Optimum enhancements in mechanical properties (tensile, flexural and impact strengths) were also noticed.

Thermo-mechanical properties of epoxy Sisa/Jute hybrid composites was investigated by [7]. The samples were produced using hand lay-up technique and the thermo-mechanical properties including storage modulus, loss modulus and damping parameter were evaluated at a temperature range of 30-200 °C. The hybrid composite with 50 % of sisal fibre content gave the optimum values of storage and loss moduli. Mohammed et al. [8] investigated the effects of fibre size and fibre content on the mechanical and physical properties of mengkuang reinforced thermoplastic natural rubber hybrid composite. The composites were produced by blending high density polyethylene/natural rubber in the ratio of 60:40 using fibre size of 125, 250, and 500 µm at fibre loading of 10, 20 and 30 % respectively. The maximum tensile strength and modulus were given at 20 % fibre loading of size 250 µm, while the impact strength decreased gradually with increase in percentage of fibre content at fibre size of 125 and 250 µm. The lowest water intake was given at 10 % fibre loading for all the sizes investigated.

It is clear from the literature surveyed that hybridization provides flexibility by tailoring the material properties according to particular requirements. Hybrid composites appear to be a weighted sum of the contributions of the individual components in which there is a balance between their advantage and disadvantage.

The present study is a contribution to this field hybridization of composites by investigating the mechanical and thermo-mechanical properties of hybrid composites produced from palm kernel fibres and palm kernel shells using epoxy resin as matrix.

## **Materials and Methods**

### **Preparation of hybrid composite**

Palm kernel shells (PKS) and palm kernel fibres (PKF) were collected from a dump site in Makurdi, Nigeria. The wastes were thoroughly washed and sun-dried for 10 hours after which they were ground into particulates and sieved into three different sieve sizes of 75 µm, 150 µm and 300 µm. The PKF and PKS particulates were then blended in the weight ratios (fibre/kernel) of 50:50 and maintained throughout the formulation process. The blended particulates were then weighed and thoroughly mixed with previously weighed epoxy resin matrix. Formulation of the composites was divided into three main composition ratios (epoxy/PKF/PKS). Each composition ratio was again divided into three; according to grain size of the particulate material (Table 1). From each particulate size, five samples tagged A, B, C, D and E were produced and coded as; A(90:5:5); B(80:10:10); C(70:15:15); D(60:20:20); and E(50:25:25).

**Table 1.** Percentage composition of palm kernel fibre-palm kernel shell particulate epoxy hybrid composites

Grain Size	Material	Sample/ Weight %				
		A	B	C	D	E
75 $\mu\text{m}$	Palm kernel fibre	5	10	15	20	25
	Palm kernel shell	5	10	15	20	25
	Epoxy	90	80	70	60	50
150 $\mu\text{m}$	Palm kernel fibre	5	10	15	20	25
	Palm kernel shell	5	10	15	20	25
	Epoxy	90	80	70	60	50
300 $\mu\text{m}$	Palm kernel fibre	5	10	15	20	25
	Palm kernel shell	5	10	15	20	25
	Epoxy	90	80	70	60	50

Composites were produced at 10wt%, 20wt%, 30wt%, 40wt% and 50wt% particulate reinforcement by dispersed hand lay-up technique. The mixture was then dispersed on a wooden plate mould measuring 200 mm x 150 mm x 5 mm using a hand roller to properly roll the mixture in order to remove trapped air. The mould cavity was polished with a thin layer of silicon oil solution which acted as a releasing agent. This procedure was repeated until the desired thickness was obtained. Thereafter a pressure of 73 kN was applied from the top of the closed mould and maintained for 72 hrs at room temperature. The produced samples were removed and allowed to fully cure under atmospheric conditions for 35 days [9]

### Evaluation of the Hybrid Composites

#### Density

The density of the hybrid samples was determined using the liquid displacement method based on Archimedes principle as per ASTM D 792 – 08 standards. The size of the specimen used was 20 mm x 20 mm x 5 mm from each sample. The samples were first weighed on a precision balance with precision nearest to 0.0001g and recorded. Each sample was then immersed inside 1mL of water in a graduated beaker. The difference between the final and initial level of water was used to determine the volume of water displaced, which was equal to the volume of the specimen immersed. This volume was recorded for each sample and using equation (1):

$$\text{Density} = \frac{M}{V} \text{ (g/cm}^3\text{)} \quad (1)$$

Where M is the mass of the composites, and V is the volume of the samples.

#### Water absorption test

The effect of water absorption on PKS/PKF particulate/epoxy hybrid composite was investigated in accordance with ASTM D-570. The specimen size 20 mm x 20 mm x 5 mm was weighed to an accuracy of  $\pm 0.1$  mg at room temperature using a digital weighing balance. Water absorption test was conducted by immersing the composite specimens in distilled water contained in plastics cups at room temperature for a total period of 288 hours [9]. The samples were then removed from the water after 24 hours one after the other, cleaned, dried with blotting paper and weighed. The specimens were weighed at regular intervals of 24 hours for a period of 288 hours. The weights of moisture absorbed by the composites were calculated using the relationship in equation (2). Equilibrium of water intake by the samples was assumed to be reached when the daily weight gain was assumed to be less than 0.01%. The results obtained were used to plot graphs to show the trend of water intake behavior in the samples.

$$\% \text{ Moisture Absorbed} = \frac{WN - WD}{WD} \times 100\% \quad (2)$$

Where WN is the weight of the specimen after immersion and WD is the weight of the specimen before the water intake test.

#### ***Determination of tensile strength***

The tensile strength of the composite was measured using Monsanto Tensometer Type 'W'. Test samples measuring 100 mm × 10 mm × 5 mm with gauge length of 40 mm, were used. The test was conducted by gripping and pulling each specimen until catastrophic failure occurred. The load at which failure occurred was recorded. From each sample three specimens were tested and the average values of maximum tensile strength, tensile modulus and percent elongation at fracture were calculated.

#### ***Determination of flexural strength***

The flexural test was performed in accordance with ASTM D790 on a Universal materials Testing Machine 100 KN Capacity, model no. Cat.Nr.261. The 3-point bending fixture utilizing centre loading on a simple supported beam was employed. A bar of rectangular cross section measuring 100 mm × 30 mm × 5 mm was used. The rectangular bar was loaded by means of a loading nose midway between the supports. Three specimens were tested from each sample and the average value recorded. Modulus of elasticity E was calculated using equation (4).

$$E = \frac{Pl^3}{4bt^3Y} \quad (4)$$

Where P was the load (N), l was gauge length (80 mm), b, the width (mm), and Y was the deflection.

#### ***Determination of impact strength***

The impact strength of the samples was performed with the aid of Charpy Impact Testing Machine with capacity 15 J and 25 J Model No. Cat.Nr. 412 according with ASTM standard D-256. The specimen of size 80 mm x 10 mm x 10 mm was gripped horizontally as a simple beam and fractured by a blow delivered in the middle by the pendulum. Three specimens were tested from each sample and the average value of the energy required for fracture in joules was recorded.

#### ***Dynamic mechanical analysis (DMA)***

DMA was carried out with the aid of Dynamic Mechanical Analyzer model NNETZSCH DMA242E. Three samples, one from each particle size, were used. Each specimen measured 60 mm × 12 mm × 5 mm. The specimen were separately placed between two supports in the furnace of the DMA machine, heated, and forced to oscillate by means of a load applied midway between the supports at fixed frequency loadings of 2 Hz, 5 Hz, and 10 Hz. The sample response in form of storage modulus, loss modulus and damping parameters were displayed on the computer attached to the dynamic analyzer.

#### ***Scanning electron microscopy (SEM)***

Surface morphologies of samples from each of the sieve sizes were examined using Scanning Electron Microscopy (Phenom Prox. Model No. MVEO 16477830) in order to observe fibre distribution in composite and interface interaction between fibre and polymer resin. The samples were properly cleaned and rubbed with sand paper to remove unwanted dirt particles, dried in the air and polished with 5 nanometers thick Gold in sputter ion coater. The electron

beam of 15 kv was focused on the surface of the sample and the energy exchanged between the electron beam and the sample resulted in the reflection of high energy electrons. The beam current absorbed by the specimen was measured and used to create images of the specimen that were displayed on the computer monitor.

## Results and Discussion

### Effect of particulate reinforcement and particle size on density

The effect of particulate reinforcement and particle size on density of the produced composites is presented in Fig. 1. The figure shows a steady drop in density with increase in particulate reinforcement for all the particle sizes.

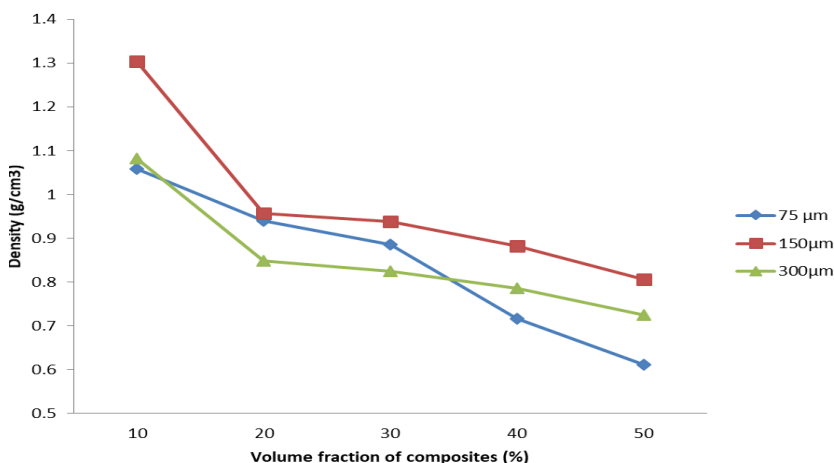


Fig. 1. Variation of density with particulate reinforcement

With increase in fibre loading from 10 – 50 % and the particle size of 75 μm has the lowest densities (0.612 -1.058 g/cm<sup>3</sup>) compared to that of 150 μm (0.806 to 1.304 g/cm<sup>3</sup>) and 300 μm (0.806 to 1.304 g/cm<sup>3</sup>). This behaviour is in agreement with [10] for composites produced from bagasse – glass fibre and similar to that reported by [11] who stated that the decrease in density may be due to light in weight of reinforcement or fibres that occupied substantial amount of space. This behaviour was attributed to the fact that for smaller particle sizes compressibility is higher due to higher porosity. These density values agreed with the values of 1.04 (15 % fibre loading), 0.99 (20 % fibre loading) and 0.80 (30 % fibre loading) g/cm<sup>3</sup> obtained by [10].

### Effect of particulate reinforcement and particle size on water absorption

Figs. 2-4 show the effect of particulate reinforcement and particle size on water absorption of the composites for three different particle sizes (75, 150, and 300 μm). It is evident from the graph that the initial rate of water uptake (i.e. percentage gain in water absorption) increases with particulate reinforcement for all particle sizes. This behavior has been explained on the basis of the hydrophilic nature of fibres and the greater interfacial area between the fibres and the matrix which leads to enhancement of micro void formation in the matrix resin [10]. The amount of water uptake by epoxy resin is almost negligible as it is hydrophobic in nature. The percentage gain in moisture absorption increases rapidly for the 1<sup>st</sup> and 4<sup>th</sup> day until it approaches saturation point. It has also been observed that the percentage of water absorption also increases with increasing particle size. For example, at 10 wt% particulate reinforcement, composites produced with 300 μm absorbed the highest moisture followed by those with 150 μm and then those with 75 μm. This pattern is consistent at all particulate reinforcement levels and is attributed to the high

level of cellulose content of palm wastes. The high level of cellulose content in the particulate reinforcement contributes to more water penetrating into the interface through the micro cracks induced by swelling of fibres thereby creating swelling stresses. Eng *et al.* [4] explained that as the composite cracks and gets damaged, capillary and transport mechanism via micro cracks become active. The capillary mechanism involves the flow of water molecules along fibre-matrix interfaces and a process of diffusion through the bulk matrix. The process is very similar to a Fickian diffusion process. The water molecules actively attack the interface, resulting in de-bonding of the fibre and the matrix.

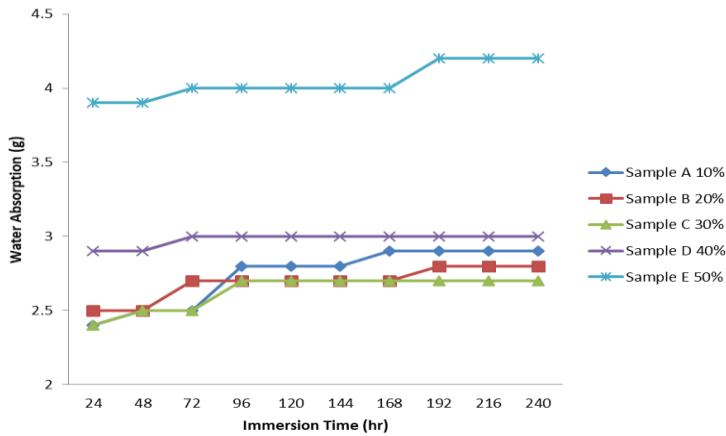


Fig. 2. Water absorption curve for varying particulate reinforcements of composites produced with 75 µm particle size

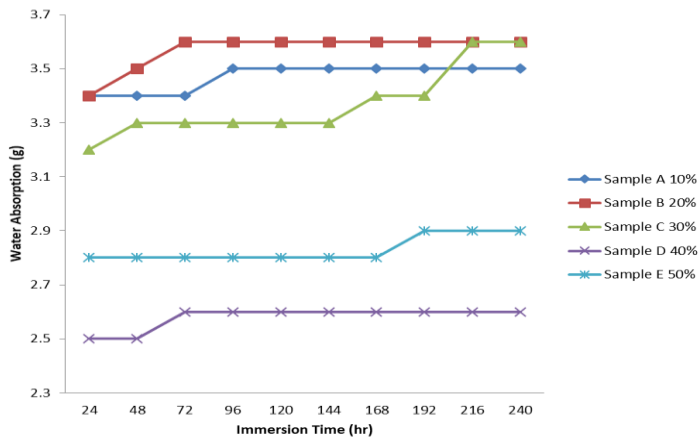


Fig. 3. Water absorption curve for varying particulate reinforcements of composites produced with 150 µm particle size

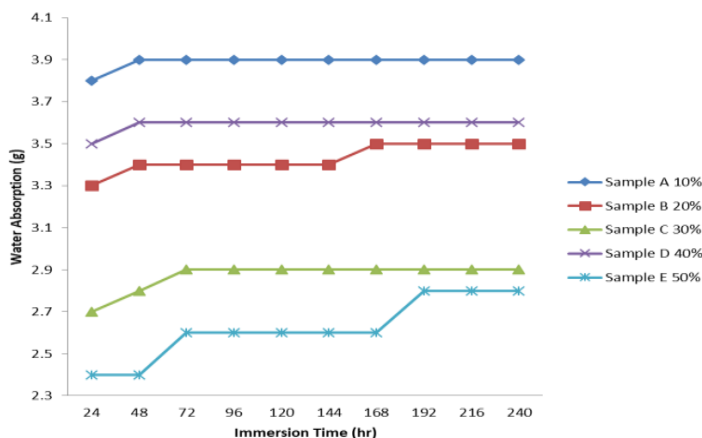


Fig. 4. Water absorption curve for varying particulate reinforcements of composites produced with 300 μm particle size.

**Effect of particulate reinforcement and particle size on mechanical properties**

**Tensile properties**

The effects of particulate reinforcement and particle size on ultimate tensile strength, modulus of elasticity and elongation are represented in Figs. 5, 6 and 7 respectively. The mechanical performance of the composites was affected by the amount of reinforcement. Figure 5 reveals that for composites produced with particle size of 75 μm, there was steady increase in tensile strength for up to 40 wt% reinforcement. However, at 50 wt% particulate reinforcement, a sharp drop in tensile strength was noticed. The drop at 50 wt% reinforcement may be due to improper adhesion of the fibres to the matrix as explained by [12]. The authors maintained that as the fibre content increases, instead of dispersion, the gathering of fibres takes place and the resin cannot wet the fibres due to non-entrance of resin in-between two adjacent fibres. Fibre wettability has also been shown to affect tensile strength of composites [5]; that good fibre dispersion promotes good interfacial bonding, reducing voids and ensuring that fibres are fully surrounded by the matrix.

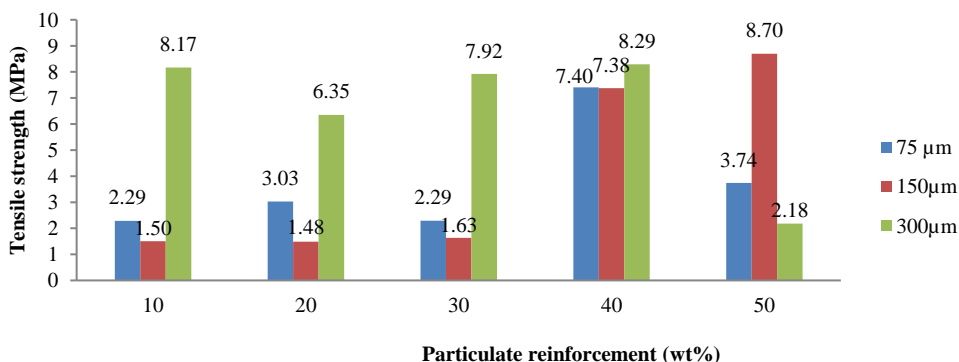


Fig. 5. Effect of particle size and particulate reinforcement on tensile strength of the composites

In composites produced with 150 μm particle size, reinforcement of up to 30 wt% was not effective in increasing the tensile strength. However, at 40 and 50 wt%, there was significant increase in tensile strength. Maximum strength of 8.696 MPa was observed in composites reinforced with 50 wt% particulate. The results also show that reinforcement with particulate was

effective in increasing the tensile strength of samples produced with 300 μm particle size. This may be due to better fibre distribution in the matrix, as the bond between fibre and matrix often dictates improved properties of composites. Effective loads are transferred between fibre and matrix resulting in increased tensile strength [13].

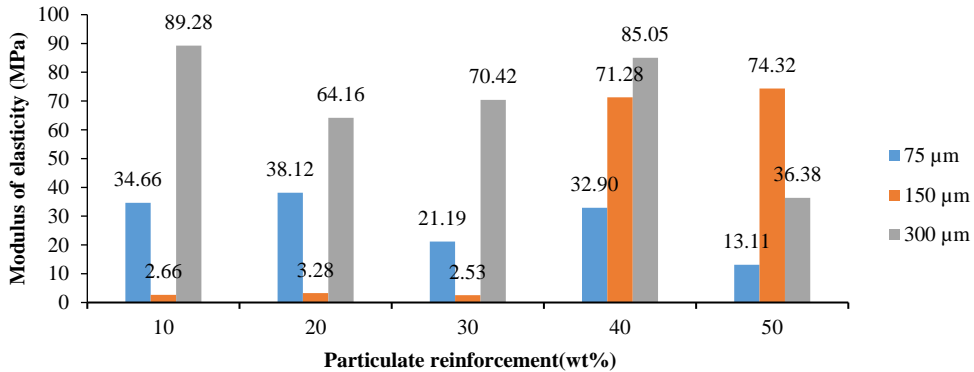


Fig. 6. Effect of particulate reinforcement and particle size on modulus of elasticity

In Fig. 6, the effect of particulate reinforcement and particle size on the modulus of elasticity of produced composites is presented. The results show similar behaviour as those for tensile strength i.e. reinforcement of up to 30 wt% was not effective in increasing the modulus. Again at 40 and 50 wt%, there was significant increase in the modulus of elasticity. The results also show that reinforcement with particulate was effective in increasing the modulus of elasticity of samples produced with 300 μm particle size. This behaviour agrees with [14] where it was found that composites developed from bone ash and bone particulate reinforced polyester were observed to behave in the same manner.

Young’s modulus of the produced hybrid composites from 75 μm particle size varied from 13.115 – 38.117 MPa for produced composites. Modulus of elasticity of the produced composites from 150 μm particle size varied from 2.530 – 74.322 MPa, while that from 300 μm varied from 36.3817-89.2768 MPa. The highest young modulus of 89.27 MPa at 10 % fibre loading was achieved, implying that the composite can be used in a situation where stiffness is the required property.

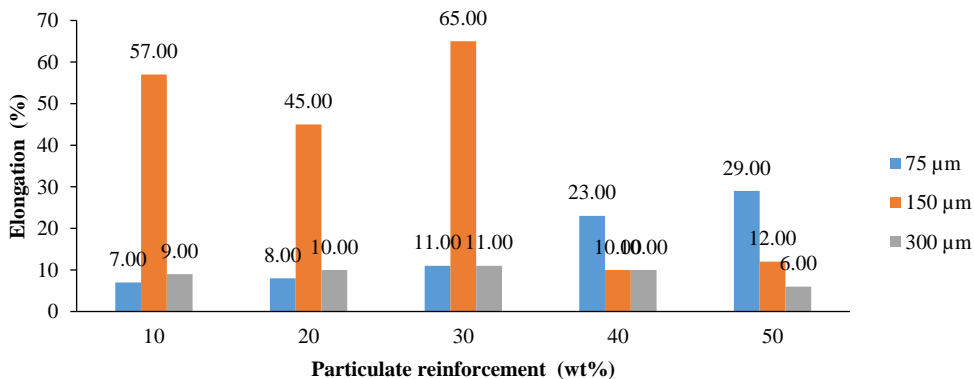


Fig. 7. Effect of particulate reinforcement and particle size on elongation



Percentage elongation (Fig. 7) increased steadily with particulate reinforcement for composites produced from 75  $\mu\text{m}$  particle size. There were variations in percentage elongation among the composites with increased fibre loading. The effect of sieve size on the elongation of produced composites shows an increase in elongation from 75 to 150  $\mu\text{m}$  size, but drops sharply to sieve size of 300  $\mu\text{m}$ . This behavior agrees with [15] where percentage elongation of periwinkle shells increases with increasing particle size but drops further as the particle size was increased. The reduction in elongation as the particle size increases could be attributed to controlled mobility of matrix by filler particles, and as the particle size of the filler increases there is reduction in total surface area available for matrix–filler interaction. The highest percentage elongation of 29 % at 50 % fibre loading was obtained from 75  $\mu\text{m}$ .

### ***Impact strength***

Fig. 8 shows the effect of particulate reinforcement and particle size and on the impact strength of the produced composites. There was a variation in impact energy among the composites with increased particle size and fibre loading, and this may be due to voids and non-proper bonding that existed in the produced composites. Composites from 300  $\mu\text{m}$  particle size presented a significant increase in impact strength when compared to composite with finer particle sizes (75 and 150  $\mu\text{m}$ ). This behavior is in agreement with [16] for palm kernel shell and cow bone reinforced polymer composites that gave better impact energy at high sieve size than finer particle size. This behavior can further be explained as a result of poor dispersion and distribution of the particles in the matrix. The values of impact strength obtained ranged from 4000 – 7400  $\text{J/m}^2$ , 6000 – 7500  $\text{J/m}^2$  and 4500 – 10,000  $\text{J/m}^2$  from 75, 150 and 300  $\mu\text{m}$  particle sizes respectively. The highest impact strengths value of 10,000  $\text{J/m}^2$  was obtained from composite with 300  $\mu\text{m}$  sizes at 20 % fibre loading. The values of impact strength were better than the values of 22.05, 24.32 and 27.01  $\text{J/m}^2$  at 10 wt % bagasse based composite, 20 wt % at bagasse-glass fibre composites and 30 wt % at bagasse-glass fibre respectively reported by [17]. The values were also better than value of 9.3  $\text{J/m}^2$  for wooden short fibre reinforced composite and 3.94 -4.7  $\text{J/m}^2$  for sisal reinforced polymer composites for 10, 15 and 20 wt % reported by [18]. From these results, it is obvious that structural components such as car bumpers could be developed from natural composites with 20 wt% PKS-PKF fibre loading from 300 and 150  $\mu\text{m}$  particle sizes.

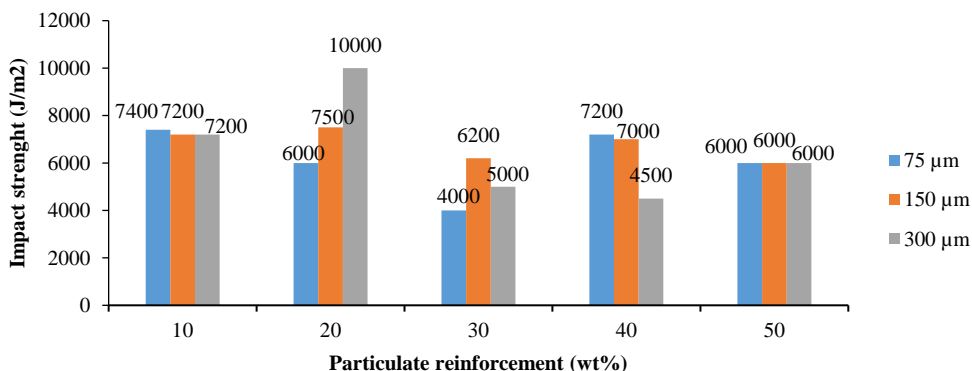


**Fig.8.** Effect of particulate reinforcement and particle size on impact strength

### ***Flexural strength***

The effect of particle size and particulate reinforcement on the flexural strength of the produced composites is shown Fig. 9. There was variations in flexural properties among composites with increased particle size and fibre loading. The flexural strength decreased from 75 to 150  $\mu\text{m}$  and raised to 300  $\mu\text{m}$  particle size. The flexural strengths from 75, 150 and 300

$\mu\text{m}$  particle size hybrid composites respectively, varied from 4.468 – 8.033 MPa, 1.277 – 8.508 MPa, and 4.726 – 10.7760 MPa, and the optimum values at 10 % fibre loading were 8.0329 MPa, and 10.7760 MPa respectively, from 75 and 300  $\mu\text{m}$  particle sizes. This behaviour agrees with [19], and similar to the finding by [20]. This may be attributed to the inability of the fibre to support stresses transferred from the polymer matrix and poor interfacial bonding that generates partial spaces between fibre and matrix materials which gave rise to weak structure [21].

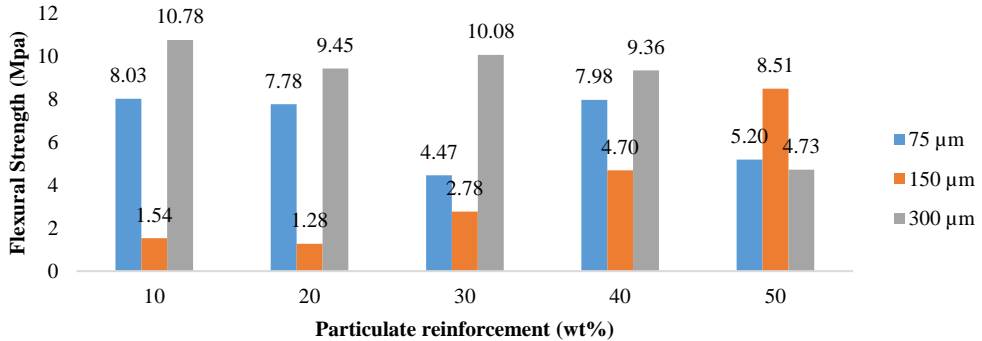


Fig. 9. Effect of particulate reinforcement and particle size on flexural strength

**Thermo-mechanical properties**

**Dynamic Mechanical Analysis (DMA)**

Figs. 10-13 show the storage modulus ( $E'$ ), loss modulus, and damping factor at different frequencies (2.0, 5.0 and 10 Hz) as a function of temperature for the composites produced from 75, 150, and 300  $\mu\text{m}$  sieve size respectively; while Figure 13 gave that of 100 % epoxy for the purpose of comparison. The figures revealed that storage modulus ( $E'$ ) decreased with increasing temperature and frequency, and the decrease in storage modulus was due to loss in stiffness of the fibre, as the trend was in consonance with that of [22], [7], and [20]. The result of the peaked storage modulus indicated that the composite with 10 % fibre loading and 300  $\mu\text{m}$  gave the highest storage modulus of 1465.7431 MPa at frequency of 10 Hz. The values of storage modulus obtained at different frequencies for pure epoxy were lower than the values obtained by the produced composites. This is due to the incorporation of PKS-PKF tends to resist mobility of the matrix.

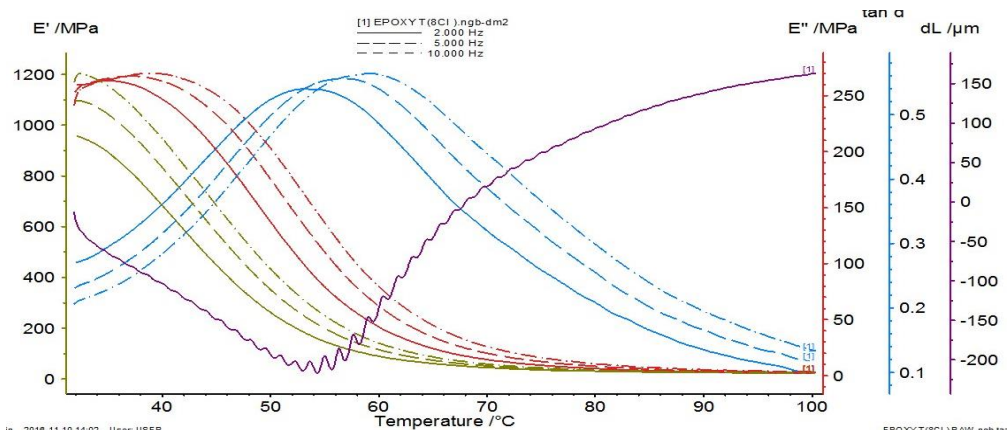
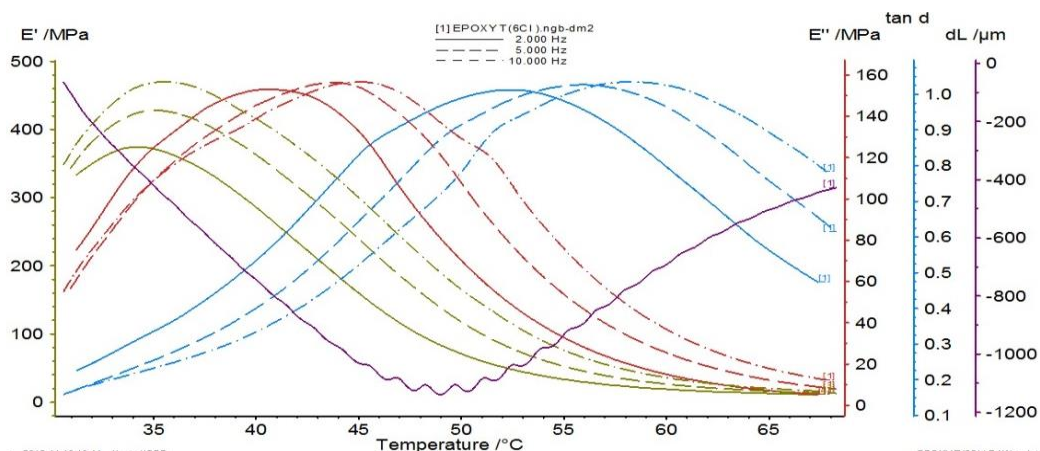
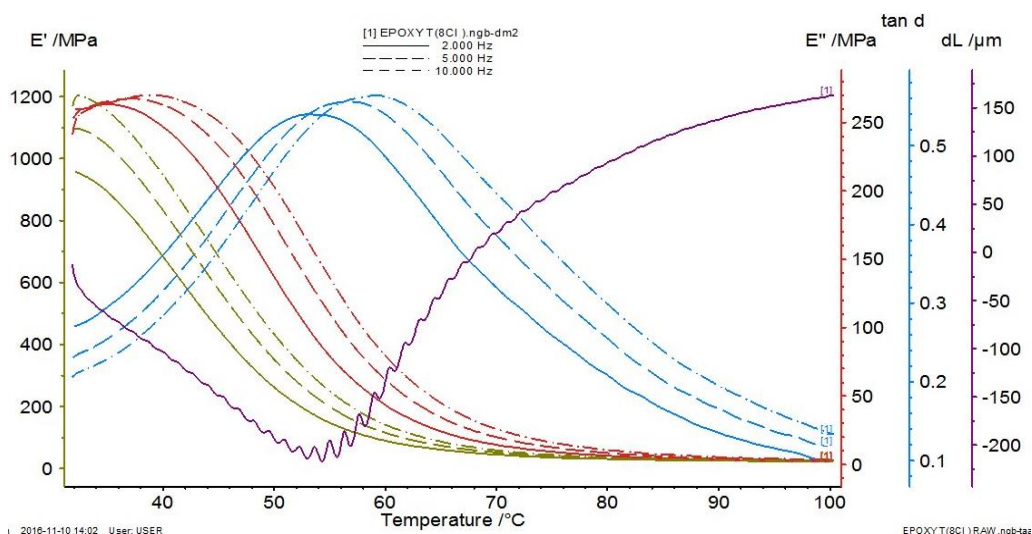


Fig. 10. Combination of storage modulus, tand, dL with temperature for composite with 40 % PKS-PKF and Particle Size of 75  $\mu\text{m}$



**Fig. 11.** Combination of storage modulus, tan Delta, dL with temperature for composite with 50 % PKS-PKF and particle size of 150 μm



**Fig. 12.** Combination of storage modulus, Tan d, dL with temperature for composite with 10 % PKS- PKF and particle size of 300 μm

The values of loss modulus as shown in Figs. 10-13 for the three produced composites and the epoxy respectively, were found to increase with increasing temperature up to glass transition temperature and then decreased. The maximum  $E''$  value found was 180.1887 at frequency of 2.0 Hz from 300 μm composite with fibre loading of 10 wt % PKS-PKF, and the lowest  $E''$  of 156.5019 at frequency of 10 Hz for pure epoxy. The peaks of loss modulus composites were found to displace to higher temperatures indicating a reduction in the chain flexibility. The highest glass transition temperatures of 63 °C was observed at 50 % fibre loading.

The effect of damping parameters on the produced composites from 75, 150, and 300 μm sieve size and epoxy respectively, as a function of temperatures at various frequencies are presented in Figs 10-13. It was observed that damping factor increased with increase in temperature and goes at maximum level in transition region and decreases in rubbery region. The high damping peaks in a composite indicate that once the deformation is induced in a material; the material will not recover its original shape [2]. The maximum value of tan d among the three composites investigated was 0.9057 from 300 μm composite with 10 wt % PKS-PKF) at frequency of 5.00 Hz and the lowest

value of  $\tan \delta$  was 0.5395 for composite with composition (40 wt% PKS-PKF) from 75  $\mu\text{m}$  at frequency of 2.00 Hz. The lower values of  $\tan \delta$  obtained by the produced composite with 40 % PKS-PKF as compared to 1.034 for pure epoxy. This implies that the samples exhibited good load capacity and strong adhesion between fibres and matrix [2].

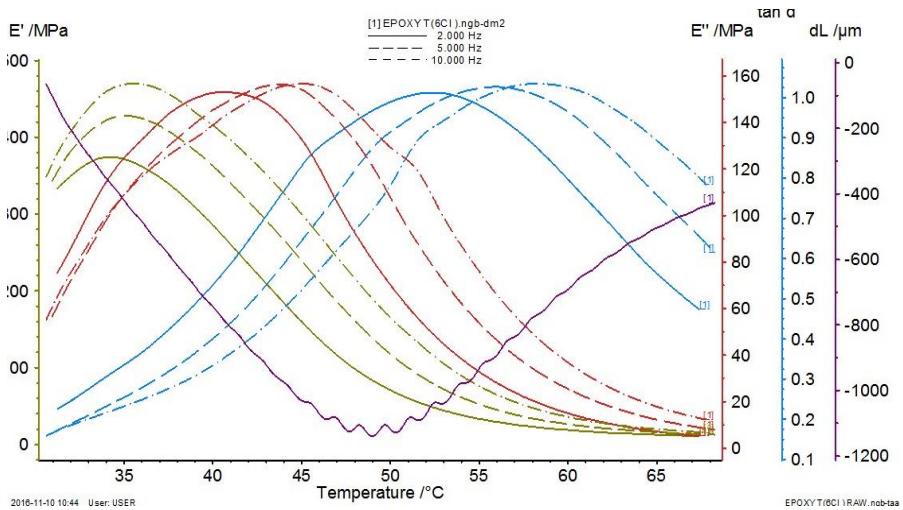


Fig. 13. Combination of Storage Modulus, Tan  $\delta$ , dL With Temperature for 100% Epoxy

**Scanning Electron Microscopy (SEM)**

Fig. 14-17 present the microstructure and fibre distribution composites from 75, 150 and 300  $\mu\text{m}$  particle size; and pure epoxy respectively. It was observed that better fibre/matrix bonding exist in the produced composites with 40 % and 10 % PKS-PKF fibre loading ( see Figure 15 (a) and 17a ) compared to composite with 50 % PKS-PKF fibre loading shown on (Figures 16 (a),). Fibre/matrix de-bonding was evident in the produced composite from 150  $\mu\text{m}$  with 50 % PKS-PKF fibre loading as there was fibre pull outs and de-bonding as most of the fibres were clearly visible as compared to pure epoxy shown in Fig. 17 at the same magnification. This was confirmed by Fig 16 (b) with non-homogeneous dispersion of randomly distributed particles with distributed particles with different dimensions characterized by 1.07-15.00  $\mu\text{m}$  in diameter.

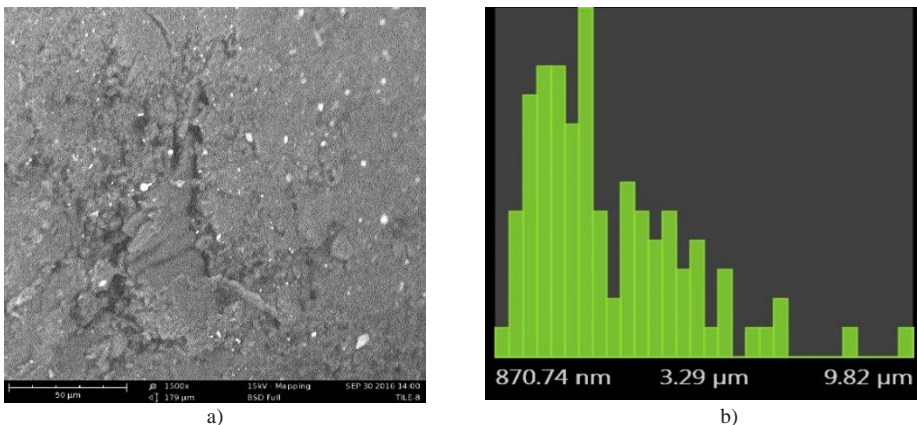
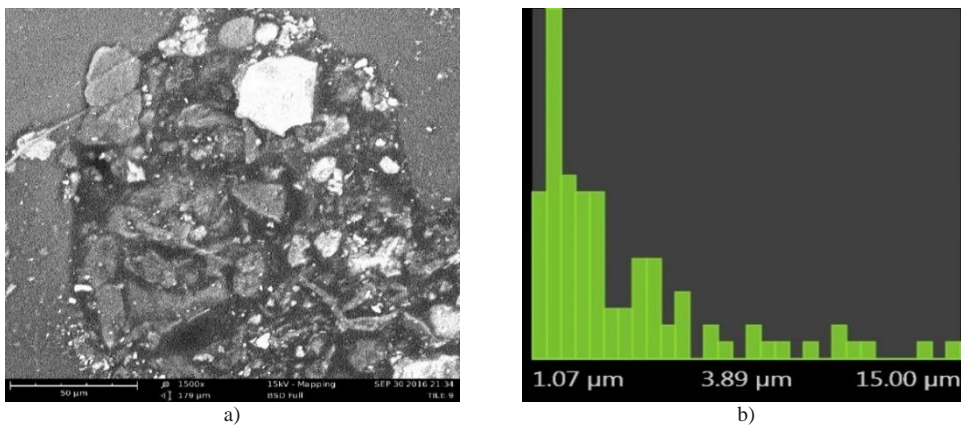
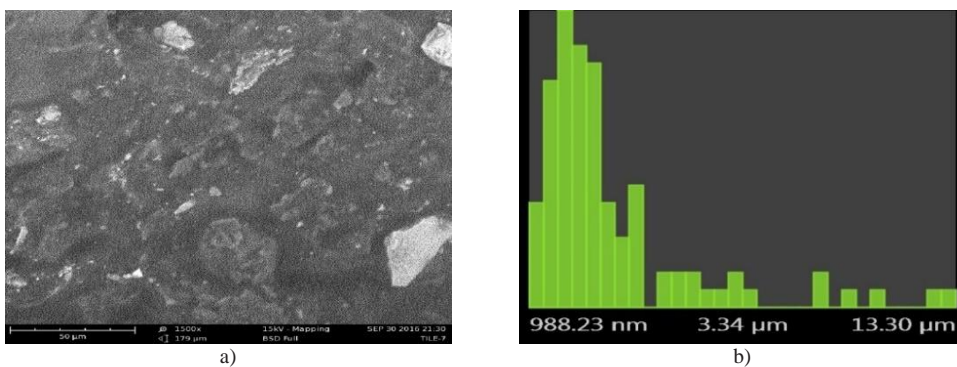


Fig. 14. a) SEM microstructure and b) Fiber histogram of composite of composite with 40 % PKS- PKF and particle size of 75  $\mu\text{m}$



**Fig. 15.** a) SEM microstructure and b) Fiber histogram of composite of composite with 50 % PKS- PKF and particle size of 150 μm



**Fig. 16.** a) SEM microstructure and b) Fiber histogram of composite of composite with 10 % PKS- PKF and particle size of 300 μm

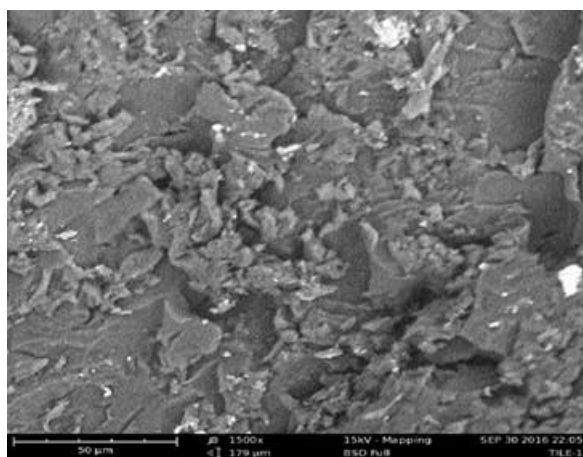


**Fig. 17.** SEM microstructure of 100 % epoxy

The composite from 300 μm with 10 % PKS-PKF as shown in Fig. 17 was observed to have matrix rich regions because of low fibre content. The fibre distribution 75 μm for produced composite with composition from particle sieve size with 40 % PKS-PKF drawn in terms of histogram varied from 870.74 nm – 9.82 μm. As histogram measures composite fibre fineness,

and the evenness of distribution of that fineness. The fibre distributions for composite with with 50 % PKS-PKF fibre loading from 150  $\mu\text{m}$  varied from 1.07 – 15.00  $\mu\text{m}$ . This implies that finest fibre was 1.07  $\mu\text{m}$  to the left hand of the figure and coarser 15.00  $\mu\text{m}$  to the right. The most fibres were observed to gather most at 1.07  $\mu\text{m}$  as compared to 870.74 nm and 9.82  $\mu\text{m}$  for composite 40 % PKS-PKF. The fibre distribution of 988.23 nm – 13.30  $\mu\text{m}$  for composite (10 % PKS-PKF) was obtained from 300  $\mu\text{m}$  particle size.

## Conclusion

The following conclusions were drawn from the study:

The particle size and fibre loading affect the thermos-mechanical and physical properties of the hybrid composites produced from palm kernel fibres and palm kernel shells.

The optimum Young modulus value and flexural strength value of 89.277 MPa and 10.7760 MPa respectively were obtained from sample A (300  $\mu\text{m}$  particle size. with 10 % fibre loading. The optimum value of impact strength was given by sample B (300  $\mu\text{m}$  particle size) with 20 % fibre loading was 10000 J/m<sup>2</sup>. These values were in agreement with other composites produced from some natural fibre reported in literature.

Dynamic properties of the hybrid PKS-PKF composites were found to depend on particle size and fibre loading. The storage modulus as well as loss modulus was found to be higher for hybrid composite than pure epoxy.

The physical properties such as density, and water absorption were found to be influenced by particle size and fibre loading. The overall result of water absorption showed that particle size of 300  $\mu\text{m}$  absorbed the highest water, while particle size of 75  $\mu\text{m}$  had the least density.

## References

- [1] G. Venkatachalam, , A.S. Gautham, K.V. Vijay, B.R. Chandan., G.P. Prabaharam, R. Dasarath, *Evaluation of tensile strength of hybrid fibre (jute/gongura) reinforced Hybrid polymer matrix composites*, **Materials Science and Engineering**, **87**, 2015, doi:10.1088/175-899X/87/1/012108.
- [2] L.A. Pothan., C.N. George, M.J John, S.N. Thomas, M.J. John, S. Thomas, *Dynamical and dielectric behavior of banana-glass hybrid fibre reinforced polyester composites*, **Composites Science and Technology**, **68**, 2010, pp. 287-298.
- [3] D. Romomazini, A. Lavoratti, H.L. Ornaghi, S.C. Amico, A.J. Zattera, *Influence of fibre content on the mechanical and dynamic mechanical properties of glass/ramie polymer composites*, **Materials and Design**, **4**, 2013, pp. 9-15.
- [4] C.C. Eng., N.A. Ibrahim, N. Zainuddin, H. Ariffin, W.M.Z.W Yunus, *Impact strength and flexural properties enhancement of Methacrylate silane treated oil palm nesocarp fibre reinforced biodegradable hybrid composites*, **Hindawi publishing corporation, the scientific World Journal**, 2014, pp. 1-8. <http://dx.doi.org.10.1155/2014/213180>.
- [5] K.L. Pickering, A.M.G. Efendy, T.M. Le, *A review of recent developments in natural fibre composites and their mechanical performance*, **Composites**, **83**, 2016, pp. 98-112.
- [6] R.P. Venkatesh, K. Ramanathan, V.S. Raman, *Tensile, impact and water absorption of natural fibre reinforced polyester hybrid composites*, **Fibres and Textiles in Europe**, **24 (3)**, 2015, pp. 90-94.
- [7] M.K. Gupta, R.K. Srivastava, *Tribological and dynamic analysis of epoxy based hybrid sisal/jute composite*, **Indian Journal of Engineering and Materials Sciences**, **23**, 2016, pp. 37 44.
- [8] W.Z.W. Muhamed, A. Baharum , I. Ahmed, I. Abdullah, N.E. Zakaria, *Effects of fiber size and fiber content on the mechanical and physical properties of mengkuang reinforced*

- thermoplastic natural rubber composites*, **BioResources**, **13** (2), 2018.
- [9] M. Jawaid, H.P.S.A. Khalil, A.A. Bakar, A.R. Hassan, Dunyani, *Effect of fibre loading on the mechanical and thermal properties of oil palm epoxy composites*, **Journal of Composites Material**, **47**(13), 2012, pp. 1633-1641.
- [10] M. Tewari, V.K. Sigh, P.C. Gope, A.K. Chaudhary, *Evaluation of mechanical properties of bagasse-glass fibre reinforced composite*, **Journal of Mater. Environ. Sci.**, **3**(1), 2012, pp.171-184.
- [11] L.M. Dagwa, P.F. Builders, J. Achebo, *Characterization of palm kernel shell powder for use in polymer matrix*, **12**(4), 2012, pp. 88.
- [12] G. Das, S. Biswas, *Physical, mechanical and water absorption behaviour of coir fibre reinforced epoxy composite filled with Al<sub>2</sub>O<sub>3</sub> particulates. 5<sup>th</sup> International Conference on processing and Characterization*, **Materials Science and Engineering**, 2016, 115, doi:10.1088/1757-899X/115/1/012012.
- [13] S-Y. Fu, X-Q. Feng, B. Lauke, Y-W. Mai, *Effects of particle size, particle/matrix interface adhesion and particle loading on mechanical properties of particulate-polymer composites*, **Composites part B. Engineering**, **39**, 2008, pp. 933-961.
- [14] I.O. Oladele, *Development of bone ash and bone particulate reinforced polyester composites for biomedical applications*, **Leonardo Electronic Journal of Practices and Technologies**, **22**, 2013, pp. 15-26.
- [15] I.O. Michael, I.A. Fidelis, U.U. Ikpi, *Mechanical Properties of Hybrid Periwinkle and Rice Husk Filled CNSL Composite*, **International Journal of Nano and Material Sciences**, **1**(2), 2012, pp. 4-80.
- [16] Mayowa, A., O.K. Abubakre, S.A. Lawal, R. Abdulkabir, *Experimental investigation of Palm Kernel Shell and Cow Bone Reinforced Polymer Composites for Brake and Pad Production*, **International Journal of Chemistry and Materials research**, **3** (2), 2015, pp. 27 -40.
- [17] R.K.Upadhyay, M. Ali, G.D Gautam, *Tensile and impact strength of natural fibre reinforced polymer composites for building structural application*, **Journal of Civil Engineering and Environmental Technology**, 2015, pp. 81-84.
- [18] J. Zhang, Z. Wang, X. Wang, W. Liang, L. Zhou, *Automatic generation of random distribution of fibers in long-fiber-reinforced composites and mesomechanical simulation*, **Mater. Des**, **32**, 2011, pp. 885-891.
- [19] A.I. Al-Mosawi H.K. Ammash, A.J. Salaman, *Properties of Composite Materials Data book 2nd edition*, 2012, **Lambert Academic Publishing LAP**.
- [20] O. Shakuntala, G. Raghavendra, A.S. Kumar, *Effect of filler loading on mechanical and tribological properties of wood apple shell reinforced epoxy composite*, **Advances in Materials Science and Engineering**, 2014, pp. 1-9, <http://dx.doi.org/10.1155/2014/538651>.
- [21] G.P. Thomas, *Resin transfer moulding (RTM)- Methods benefit and Applications*, 2013, pp. 45-113, Accessed at [www.azom.com/article.aspx](http://www.azom.com/article.aspx).
- [22] A.O.A. Ekhlas, *The mechanical properties of natural fibre composites. PhD thesis submitted to the Faculty of Engineering*, Swinburne University of Technology, Sweden, 2013, pp. 254.

---

Received: May 07, 2019

Accepted: July 23, 2019